

Metabolomics diagnostic approach to mustard airway diseases: a preliminary study

BiBi Fatemeh Nobakht Mothlagh Ghoochani ¹, Rasoul Aliannejad ^{2*}, Afsaneh Arefi Oskouie ³, Mostafa Rezaei-Tavirani ⁴, Shiva Kalantari ⁵, Mohammad Taghi Naseri ⁶, Alireza Akbarzadeh Baghban ⁷, Hadi Parastar ⁸, Ghazaleh Aliakbarzadeh ⁹

¹ Department of Basic Medical Sciences, Neyshabur University of Medical Sciences, Neyshabur, Iran

² Pulmonary Department, Shariati Hospital, Tehran University of Medical Sciences, Tehran, Iran

³ Department of Basic Sciences, Faculty of Paramedical Sciences, Shahid Beheshti University of Medical Sciences, Tehran, Iran

⁴ Proteomics Research Center, Faculty of Paramedical Sciences, Shahid Beheshti University of Medical Sciences, Tehran, Iran

⁵ Chronic Kidney Disease Research Center, Labbafinejad Hospital, Shahid Beheshti University of Medical Sciences, Tehran, Iran

⁶ Department of Chemistry, Faculty of Sciences, Tarbiat Modares University, Tehran, Iran

⁷ Physiotherapy Research Center, School of Rehabilitation, Shahid Beheshti University of Medical Sciences, Tehran, Iran

⁸ Department of Chemistry, Sharif University of Technology, Tehran, Iran

⁹ Department of Chemistry, Faculty of Science, University of Tehran, Tehran, Iran

ARTICLE INFO

Article type:

Original article

Article history:

Received: May 24, 2017

Accepted: Sep 28, 2017

Keywords:

GC-MS

Metabolomics

Multivariate analysis

NMR spectroscopy

Sulfur mustard

ABSTRACT

Objective(s): This study aims to evaluate combined proton nuclear magnetic resonance (¹H NMR) spectroscopy and gas chromatography-mass spectrometry (GC-MS) metabolic profiling approaches, for discriminating between mustard airway diseases (MADs) and healthy controls and for providing biochemical information on this disease.

Materials and Methods: In the present study, analysis of serum samples collected from 17 MAD subjects and 12 healthy controls was performed using NMR. Of these subjects, 14 (8 patients and 6 controls) were analyzed by GC-MS. Then, their spectral profiles were subjected to principal component analysis (PCA) and orthogonal partial least squares regression discriminant analysis (OPLS-DA).

Results: A panel of twenty eight metabolite biomarkers was generated for MADs, sixteen NMR-derived metabolites (3-methyl-2-oxovaleric acid, 3-hydroxyisobutyrate, lactic acid, lysine, glutamic acid, proline, hydroxyproline, dimethylamine, creatine, citrulline, choline, acetic acid, acetoacetate, cholesterol, alanine, and lipid (mainly VLDL)) and twelve GC-MS-derived metabolites (threonine, phenylalanine, citric acid, myristic acid, pentadecanoic acid, tyrosine, arachidonic acid, lactic acid, propionic acid, 3-hydroxybutyric acid, linoleic acid, and oleic acid). This composite biomarker panel could effectively discriminate MAD subjects from healthy controls, achieving an area under receiver operating characteristic curve (AUC) values of 1 and 0.79 for NMR and GC-MS, respectively.

Conclusion: In the present study, a robust panel of twenty-eight biomarkers for detecting MADs was established. This panel is involved in three metabolic pathways including aminoacyl-tRNA biosynthesis, arginine, and proline metabolism, and synthesis and degradation of ketone bodies, and could differentiate MAD subjects from healthy controls with a higher accuracy.

► Please cite this article as:

Nobakht Mothlagh Ghoochani BF, Aliannejad R, Arefi Oskouie A, Rezaei-Tavirani M, Kalantari Sh, Naseri MT, Akbarzadeh Baghban AR, Parastar H, Aliakbarzadeh Gh. Metabolomics diagnostic approach to mustard airway diseases: a preliminary study. Iran J Basic Med Sci 2018; 21:59-69. doi: 10.22038/IJBMS.2017.23792.5982

Introduction

Sulfur mustard (2,2'-dichlorodiethyl sulfide, SM) is an alkylating agent that causes dose-dependent morbidities after topical or inhalational exposures. It can produce both early and late manifestations; delayed complications have been observed many years following the exposure to SM such as respiratory disorders (1, 2). Previous pathological and radiological studies have shown that bronchiolitis obliterans is the main airway disease in SM-exposed patients (3-5) and other airway diseases include bronchiectasis, tracheobronchomalacia, Tracheobronchial

stenosis (6, 7). Since SM can affect the entire set of conducting airways and small airways, ailments related to SM were named mustard airway diseases (MADs). Pathological and radiological findings demonstrated that MADs differ from chronic obstructive pulmonary disease (COPD) (7) in spite of having some similar symptoms (8). There is no common consensus about the pathophysiological basis of respiratory complications caused by SM (6). Of note, diagnostic criteria for MADs to date include imaging and bronchoscopy which are imperious and invasive methods, respectively.

*Corresponding author: Rasoul Aliannejad. Pulmonary Department, Shariati Hospital, Tehran University of Medical Sciences, Tehran, Iran. Fax: +98-2188220049, email: aliannejad@sina.tums.ac.ir

Metabolomics studies employ some analytical techniques including, nuclear magnetic resonance (NMR) (9, 10) and mass spectrometry (GC/LC-MS (11, 12)) for the identification of biomarkers and metabolic pathways altered in a variety of clinical disorders such as pulmonary diseases (13). It, like the other 'omic' approaches, provides precious clues to better understanding the mechanism of MADs.

Our group recently reported the feasibility of accurate NMR-based metabolomic prediction for both normal and severe individuals with MADs (14, 15). It is important that the performance of the identified biomarkers be confirmed using another potent multivariate analysis with different data mining algorithm as if it was analyzed in this work. Moreover, in the present manuscript, we use GC-MS to identify a more comprehensive metabolite panel than single approach (NMR spectroscopy) for severe patients with MADs. To the best of our knowledge, no GC-MS-based metabolomics analysis was performed in very severe MAD patients until now. We intended to gain knowledge of the pathophysiological basis of MADs and find potential metabolic biomarkers associated with MAD that may help in diagnosis and therapeutic strategies.

Materials and Methods

Reagents

N,O-Bis (trimethylsilyl) trifluoroacetamide (*BSTFA*) with 1% trimethylchlorosilane (TMCS), deuterium oxide (D_2O), pyridine, methoxyamine hydrochloride, and L-Norleucine were purchased from Sigma-Aldrich (Germany), and acetonitrile (HPLC grade) was purchased from Merck.

Sample collection

The present work was conducted by Shahid Beheshti University of Medical Sciences (SBMU) from July 2012 until October 2013, after approval by the SBMU medical ethnic committee. MAD patients were recruited from men attending the pulmonary division of Sasan Hospital (Tehran, Iran). These patients were exposed to SM in Iran-Iraq war (1983-1988).

Patients with MADs were selected from the "very severe" group, very severe airflow restriction was defined as forced expiratory volume in one second (FEV_1) < 30% and FEV_1 /forced vital capacity (FVC) < 70% predicted (16).

The details of patient recruitment, evaluation, inclusion and exclusion criteria, specimen collection, and handling have been previously published for the NMR part (14). In conducting this study, we combined NMR and GC-MS methods to identify a more comprehensive metabolite panel. A total of 17 MAD patients and 12 healthy controls in the NMR part and 8 MAD patients and 6 healthy controls in the GC-MS part were enrolled in this study following informed consent.

Volunteers in the control group were included on the basis of a physicians' assessment of their general

health status and only male volunteers were selected for this study. MAD patients were compared to age and gender-matched healthy controls. Of note, because of the severity of the disease, patients were taking inhaled corticosteroids (fluticasone 250–500 mg/salmeterol 25–50 mg per 12 hr).

Each whole blood sample was collected in a clean tube and was immediately centrifuged. The resultant serum was transferred into a clean tube and stored at $-80^\circ C$ until use.

NMR acquisition and data processing

The procedures for NMR spectroscopy and data processing were thoroughly explained in our previous study (14).

GC-MS acquisition

We mixed 100 μ l of serum with 300 μ l of acetonitrile. After vortexing, the mixture was left to stand for 15 min and then centrifuged (3000 rpm for 10 min at $4^\circ C$) to remove proteins. Subsequently, 100 μ l of the upper layer was transferred and evaporated to dryness in a vacuum centrifuge. Twenty μ l methoxyamine hydrochloride in pyridine (40 mg/ml) was added to each residue. Methoxymation was carried out at $30^\circ C$ for 90 min. After that, silylation was performed by adding 150 μ l BSTFA with 1% TMCS to the mixture. This solution was incubated for 90 min at $60^\circ C$.

GC-MS analysis of derivatized serum samples were performed using an Agilent 6890 GC coupled to an Agilent 5973 inert EI/CI mass selective detector (Agilent, Santa Clara, CA) with an HP-5MS capillary column (5% phenyl, 95% dimethylpolysiloxane; 30 m \times 0.25 mm i.d., 0.25- μ m film thickness, J&W Scientific) in the splitless mode. The flow of helium carrier gas was kept constant at 1.9 ml min^{-1} . The injection port was set at $250^\circ C$. Initial GC temperature was $60^\circ C$, holding for 3 min, and then elevated to $280^\circ C$ at a rate of 10 $^\circ C$ min^{-1} , holding for 6 min. The transfer-line heater, ion source temperature, and MS quadrupole temperature were set at $280^\circ C$, $150^\circ C$, and $150^\circ C$, respectively. The measurements were carried out with the electron impact ionization mode (70 eV). The full scan spectra (35-600 m/z) were acquired after a 7 min solvent delay. The dwell time for each was 150 ms ion^{-1} . Also, all samples were run with internal standard (L-Norleucine).

Data analysis for GC-MS

Data files from the GC-MS analysis were converted from the Agilent .d files to .csv format using the Chemstation software, and .csv files were then loaded into Matlab (version 6.5.1, The MathWorks, Cambridge, UK).

All GC-MS spectral data were firstly baseline-corrected using the asymmetric least squares (ALS) method (17) and the standard technique that was used for the alignment of peaks was the correlation optimized warping approach (COW) (18-20). The peak areas were subsequently normalized using L-Norleucine (internal standard).

Table 1. Characteristics of mustard airway disease patients and healthy controls in nuclear magnetic resonance experiment

	Control	Very severe
Number (n)	12	17
Anthropometric and demographic Characteristics		
Gender	male	male
Age (year)	47.84±7.67	47.88±7.79
Height (cm)	174.26±4.8	171.35±6.8
Weight (kg)	78.84±9.29	74.23±15.86
BMI (kg/m ²)	25.96±2.9	25.29±5.42
Lung function		
FEV ₁ (% predicted)	95.84±8.3	28.26±10.2 ^a
FVC (%)	89.26±8.1	40.46±15.26 ^a
FEV ₁ /FVC (%)	85.68±3.44	59.73±16.17 ^a

Values are presented as mean±SD. BMI: body mass index; FEV₁: forced expiratory volume in one second; FVC: forced vital capacity. Compared with the control group: ^a *P*<0.001

Statistical analysis

The obtained matrix from the "Data Analysis for NMR and GC-MS" section was imported to SIMCA Software Version 14.0 (Umetrics, Umeå, Sweden), where multivariate statistical analysis was performed. All spectra were mean-centered and unit variance (UV)-scaled before multivariate statistical analysis. To identify outliers and produce the data structure overview, principal component analysis (PCA) was performed on the dataset. Then, orthogonal projection to latent structures-discriminant analysis (OPLS-DA) was applied to build models and identify the differential metabolites between the two groups. The quality and reliability of the models were assessed by the parameters *R*² and *Q*² where *R*² measures the goodness of fit while *Q*² measures the goodness of prediction. Furthermore, a receiver operating characteristic (ROC) analysis generated from 7-fold cross-validation obtained using SIMCA and the area under the ROC curve (AUC) value was calculated using SPSS 16.0 (SPSS, Inc., Chicago, IL) with the 95% confidence interval as an estimate of diagnostic usefulness.

Identification of metabolites

Identification of metabolites using NMR

The metabolite resonances were identified according to signal multiplicity and assignments published in the literature such as one by Nicholson *et al.* (21) and online databases (<http://hmdb.ca>).

Identification of metabolites using GC-MS

We identified the interested peaks (the trimethylsilylated metabolites) by the Automated Mass Spectral Deconvolution System (AMDIS-version 2.71, 2012) and the NIST mass spectral library (version 2.0, 2008) based on retention time and *m/z* ratio. In the present study, compounds with match factor more than 80% were reported. Match factor indicates the similarity percentage between our spectrum and NIST mass spectral library.

Pathway analysis was performed using MetaboAnalyst

3 software (<http://www.metabolanalyst.ca/>). Twenty-eight metabolites that were significantly altered in the serum of MAD patients compared to healthy controls using NMR and GC/MS were entered into MetaboAnalyst. Significant pathways were considered with a *P*-value and false discovery rate (FDR) less than 0.05 and impact score more than 0.1.

Results

Clinical and anthropometric characteristics of participants

Demographic and pulmonary function tests (PTFs) are summarized in Table 1 (14) and Table 2 for NMR and GC-MS experiments, respectively. The healthy controls had significantly higher FEV₁, FVC, and FEV₁/FVC values compared to the MAD patients (*P*<0.001).

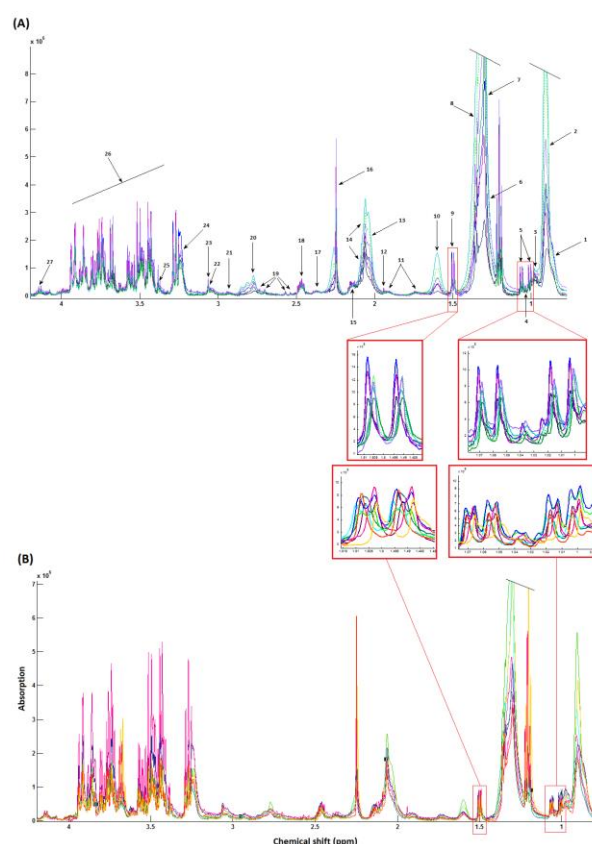


Figure 1. The Carr-Purcell-Meiboom-Gill (CPMG) sequence experiments of the serum samples from some (A) healthy controls and (B) patients ($\delta=0.7-4.2$). Red boxes in the middle illustrate magnification of valine region ($\delta=0.99-1.08$) and alanine region ($\delta=1.48-1.515$) in healthy controls and patients. The following metabolites are identified: 1, lipid: LDL $\text{CH}_3-(\text{CH}_2)_n$; 2, lipid: VLDL $\text{CH}_3-(\text{CH}_2)_n$; 3, leucine; 4, isoleucine; 5, valine; 6, lipid: LDL $\text{CH}_3-(\text{CH}_2)_n$; 7, lipid: VLDL $(\text{CH}_2)_n-\text{CO}$; 8, threonine; 9, alanine; 10, lipid: VLDL $\text{CH}_2-\text{CH}_2-\text{CO}$; 11, lysine; 12, acetate; 13, lipid: $\text{CH}_2-\text{CH}=\text{CH}$; 14, N-acetylated glycoproteins; 15: glutamate + glutamine; 16, acetoacetate; 17: glutamate; 18, glutamine; 19, citrate; 20, lipid: $\text{C}=\text{CCH}_2\text{C}=\text{C}$; 21, asparagine; 22, creatine; 23, creatinine; 24, choline; 25: proline; 26, α & β -glucose; 27, lactate

Table 2. Characteristics of mustard airway disease patients and healthy controls in gas chromatography-mass spectrometry experiment

	Control	Very severe
Number (n)	6	8
Anthropometric and demographic Characteristics		
Gender	male	male
Age (year)	45.8±4.76	46.8±7.58
Height (cm)	174.2±4.94	171.7±8.08
Weight (kg)	76.7±8.25	74.9±16.94
BMI (kg/m ²)	25.35±3.4	25.37±5.63
Lung function		
FEV ₁ (% predicted)	96.7±10.38	25.00±5.54 ^a
FVC (%)	90.2±9.13	37.8±7.92 ^a
FEV ₁ /FVC (%)	85.3±3.33	54.1±8.49 ^a

Values are presented as mean±SD. BMI: body mass index; FEV₁: forced expiratory volume in one second; FVC: forced vital capacity. Compared with the control group: ^a P<0.001

Multivariate data analysis of NMR

NMR spectra of serum samples from healthy controls and MAD patients were shown in Figures 1A and 1B, respectively.

PCA was first performed based on the normalized NMR spectral data obtained from serum; PCA score plot revealed no outliers (Figure 2A). Furthermore, no discernible clustering was observed between the MAD group and control group. The PCA score plot was characterized by the following parameters: R²X = 0.89 and Q² = 0.715.

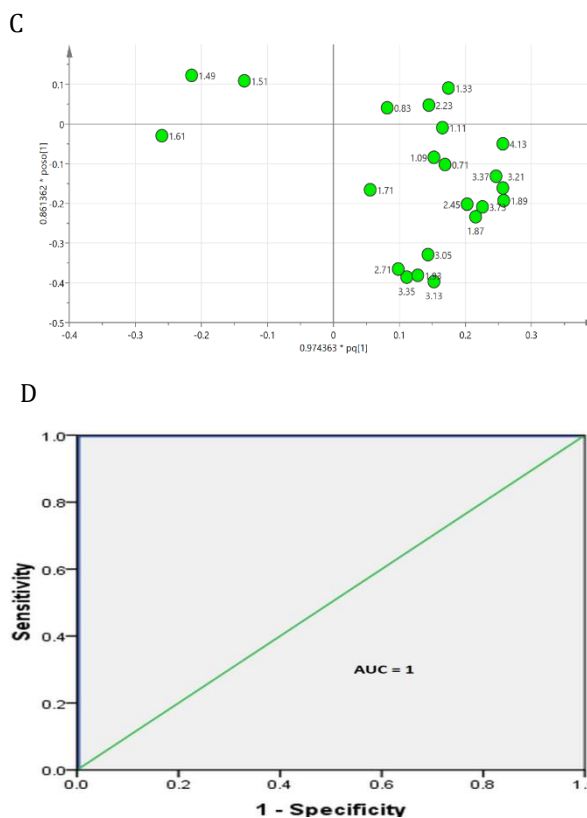
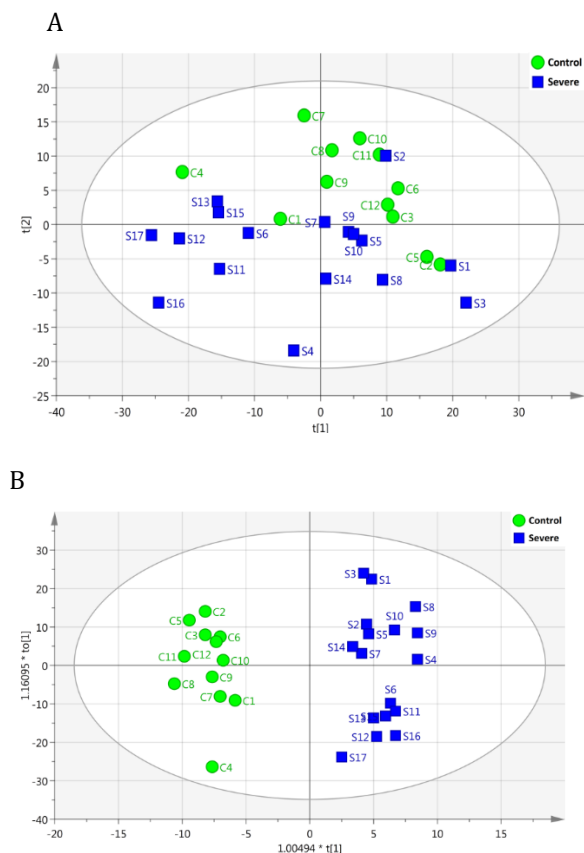


Figure 2. Metabolomic analysis of serum samples using nuclear magnetic resonance. (A) Two-dimensional PCA score plot of patients (blue box) versus healthy controls (green circle). (B) OPLS-DA score plot showing a clear discrimination between patients and healthy controls (model diagnostics were R²X= 0.749, R²Y= 0.949 and Q² = 0.873). (C) OPLS-DA loading plot showing discriminant variables between patients and healthy controls (the variables on the right are increased chemical shifts in patients and the variables on the left are decreased chemical shifts in patients, related metabolites are listed in Table 3). (D) ROC curve analysis was performed to evaluate the diagnostic performance of OPLS-DA model, AUC value was 1

OPLS-DA was then performed, which can discover the metabolic biomarkers responsible for the separation of the groups. As shown in Figure 2B, the control and MAD groups were clearly distinguished in the OPLS-DA score plot. The significant variables (chemical shifts) responsible for the discrimination between healthy controls and patients were shown as a loading plot (R²X = 0.749, R²Y = 0.949 and Q² = 0.873) of the predictive model in Figure 2C. The parameter values of the model indicated that the OPLS-DA possessed a satisfactory fit with good predictive power. The ROC curve was plotted and its corresponding AUC was 1 (Figure 2D).

In the evaluation of the MAD group against control using NMR, sixteen metabolites were significantly altered: 3-methyl-2-oxovaleric acid, 3-hydroxy-isobutyrate, lactic acid, lysine, glutamic acid, proline, hydroxyproline, dimethylamine, creatine, citrulline, choline, acetic acid, acetoacetate, and

Table 3. List of small molecular weight metabolites that play an important role in discrimination of mustard airway disease patients and healthy controls using nuclear magnetic resonance

No.	Metabolite	$\delta^1\text{H}$ (p.p.m.) ^a	Fold change	Direction of variation ^b	Metabolic pathway
1	Cholesterol	0.71, 0.83	2.1	↑	Steroid biosynthesis
2	3-methyl-2-oxovaleric acid	1.09	1.65	↑	BCAA degradation
3	3-hydroxyisobutyrate	1.11	1.84	↑	BCAA degradation
4	Lactic acid	1.33, 4.13	1.5	↑	Glycolysis
5	Alanine	1.49, 1.51	2.1	↓	Alanine metabolism
6	Lipid (mainly VLDL)	1.61	1.7	↓	Lipid metabolism
7	Lysine	1.71, 1.89, 3.73	1.57	↑	Lysine metabolism
8	Citrulline	1.87, 3.13	2.25	↑	Urea cycle
9	Acetic acid	1.93	1.96	↑	Lipid metabolism
10	Acetoacetate	2.23	1.54	↑	Synthesis and degradation of Ketone bodies
11	L-Glutamic acid	2.45	1.62	↑	Glutamine and glutamate metabolism
12	Dimethylamine	2.71	1.86	↑	Carbon metabolism
13	Creatine	3.05	1.8	↑	Glycine, serine and threonine Metabolism
14	Choline	3.21	1.9	↑	Glycerophospholipid metabolism
15	Proline	3.35	1.67	↑	Arginine and proline metabolism
16	Hydroxyproline	3.37	1.8	↑	Arginine and proline metabolism

BCAA: branched-chain amino acid; ^a Chemical shift of signal used for quantification; ^b Increased or decreased in patients compared to healthy controls

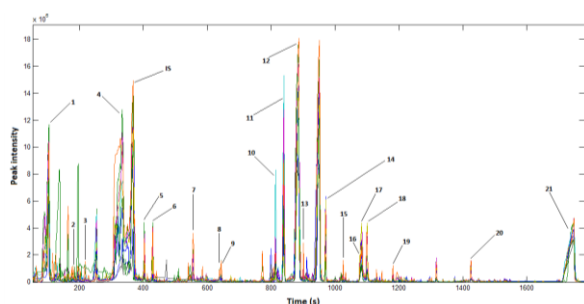


Figure 3. Representative gas chromatography-mass spectrometry total ion chromatograms of the serum samples from the two groups (patients and healthy controls) after chemical derivatization. The following metabolites are identified: 1, L-lactic acid; 2, R)-3-hydroxybutyric acid; 3, L-leucine; 4, urea; 5, L-serine; 6, L-threonine; 7, L-proline; 8, glutamine; 9, phenylalanine; 10, D-glucosylfuranoside; 11, D-galactofuranose; 12, D-glucopyranose; 13, L-tyrosine; 14, hexadecanoic acid; 15, uric acid; 16, linoleic acid; 17, oleic acid; 18, L-tryptophan; 19, arachidonic acid; 20, monostearin; 21, cholesterol

cholesterol were upregulated and alanine and lipid (mainly VLDL) were downregulated in the patient group (Table 3).

Multivariate data analysis for GC-MS

GC-MS chromatograms of serum samples from MAD patients and healthy controls were shown in Figure 3.

The resulting data were exported into the SIMCA software for multivariate analysis including PCA and OPLS-DA. The PCA score plot of GC-MS spectra data obtained from the control group and the MAD group is shown in Figure 4A ($R^2X = 0.589$ and $Q^2 = 0.332$). No outliers and no distinct PCA pattern were observed between groups.

Then, OPLS-DA was used to explore the difference between groups by incorporating the known classification. Based on the OPLS-DA model MAD patients and healthy controls were discriminated with an R^2X of 0.416, an R^2Y of 0.751, and a Q^2 of 0.239 (Figure 4B). The loading plot of the related OPLS-DA model was displayed in Figure 4C. This loading plot indicates the regions of the GC-MS spectra that are responsible for the clustering in the score plot of the serum samples. Serum metabolite biomarkers obtained from GC-MS yielded an AUC value of 0.792 in discriminating MADs from controls (Figure 4D).

A total of twelve metabolites from GC-MS analysis were identified as potential biomarkers for MADs. Differential metabolites identified from the focused metabolomic analysis suggested a significant reduction of threonine, phenylalanine, citric acid, myristic acid, pentadecanoic acid, tyrosine, and arachidonic acid in the serum of MAD patients compared to the control group but elevation of lactic acid, propionic acid, 3-hydroxybutyric acid, linoleic acid, and oleic acid (Table 4).

Metabolic pathway analysis

Metabolic pathway analysis was performed using the metaboanalyst tool. This method identified three significant metabolic pathways including aminoacyl-tRNA biosynthesis, arginine, and proline metabolism, and synthesis and degradation of ketone bodies (Figure 5A). Additionally, Figure 5B illustrated a more detailed pathway map associated with biomarker metabolites identified using both NMR- and GC/MS-based in MADs.

Table 4. Metabolites that significantly distinguish mustard airway disease patients from healthy controls using gas chromatography-mass spectrometry

No.	Metabolite	Retention time	Mass fragments	Fold change	Match factor	Direction of variation ^a	Metabolic pathway
1	Lactic acid	7.753	191,219	1.99	90.2	↑	Glycolysis
2	Propionic acid	7.946	73,147,189	2.09	83.7	↑	Fatty acid metabolism
3	3-Hydroxybutyric acid	9.913	191,233	1.76	80	↑	Synthesis and degradation of Ketone bodies
4	Threonine	12.575	73,218,117	2.74	92.8	↓	Threonine metabolism
5	Phenylalanine	16.111	218,73,192	5.25	83.3	↓	Phenylalanine and Tyrosine Metabolism
6	Citric acid	17.642	273,363,347	2.22	90.8	↓	Citric acid cycle
7	Myristic acid	17.667	117,132,285	2.19	88.4	↓	Fatty acid metabolism
8	Pentadecanoic acid	18.606	299,75,117	3.05	82.8	↓	Fatty acid metabolism
9	Tyrosine	18.657	218,73,280	3.12	92.4	↓	Tyrosine Metabolism
10	Linoleic acid	20.895	73,337,67	2.26	89.2	↑	Fatty acid metabolism
11	Oleic acid	20.972	73,339,117	1.52	93.3	↑	Fatty acid metabolism
12	Arachidonic acid	22.232	73,55,117	5.89	85.3	↓	Fatty acid metabolism

^a Increased or decreased in patients compared to healthy controls

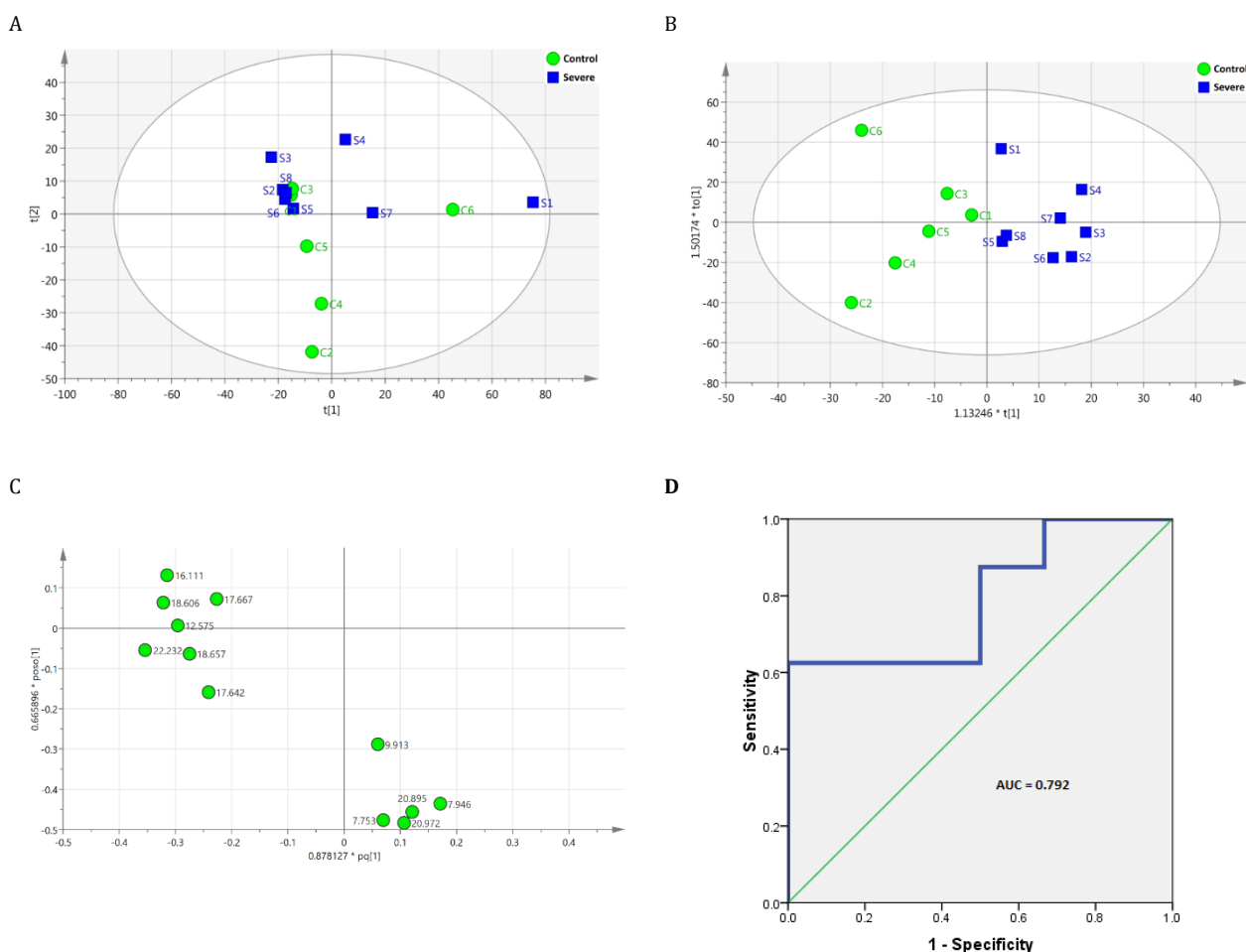


Figure 4. Metabolomic analysis of serum samples using gas chromatography-mass spectrometry. (A) Two-dimensional PCA score plot of patients (blue box) versus healthy controls (green circle). (B) OPLS-DA score plot showing a clear discrimination between patients and healthy controls (model diagnostics were $R^2X= 0.416$, $R^2Y= 0.751$ and $Q^2 = 0.239$). (C) OPLS-DA loading plot showing discriminant variables between patients and healthy controls (the variables on the right are increased retention times and the variables on the left are decreased retention times in patients, related metabolites are listed in Table 4). (D) ROC curve analysis was performed to evaluate the diagnostic performance of OPLS-DA model, AUC value was 0.792

Carbohydrates provide approximately half the energy of respiratory muscles, while the other half is predominantly from lipid or fatty acid metabolism (22). Under hypoxic condition, glycolysis occurs which leads to a significant increase in the lactic acid levels. Hypoxia can also cause activation of tissue-resident macrophages (23). Subsequently, up-regulation of pro-inflammatory cytokines including interleukin-1 (IL-1), IL-6, and tumor necrosis factor- α (TNF- α) is associated with exposure of macrophages to hypoxia (24-26). This is in agreement with previous reports that demonstrated exposure to SM may increase inflammatory cytokines such as IL-1, IL-6, and TNF- α (27-29). Furthermore, increased levels of these cytokines are associated with the induction of oxidative stress (OS); as was demonstrated in our prior study, exposure to SM elevated OS (30).

An increased level of choline was shown in the MAD group compared to the control group. Choline is released from membrane phospholipids by phospholipase D (PLD), which catalyzes the hydrolysis of phosphatidylcholine to phosphatic acid and choline during membrane breakdown after hypoxia. High PLD activity and elevated levels of serum choline have previously been associated with oxidative stress, hypoxia, and inflammation (31). The extent of choline release may reflect the severity of global tissue damage (32).

One more metabolite of interest, arachidonic acid (AA), decreased in the serum of MAD patients as compared with healthy controls. AA is a polyunsaturated fatty acid that is released from cell membranes by PLA₂ and is converted into prostaglandins during inflammation. In addition, other phospholipases such as PLC and D can cause the release of AA from membrane phospholipids (33). Study showed that short-term effect of SM is increased intracellular free calcium, which activates PLA₂ and subsequently elevates release of AA from the cell membrane (34). Moreover, it has been demonstrated that exposure to SM caused an increase in AA release from human keratinocytes (35). However, we found decreased levels of AA in the serum of MAD patients. As stated previously, patients with MAD received corticosteroids, which induce biosynthesis of a PLA₂ inhibitor that prevents the release of AA (36). Unlike AA, two more unsaturated fatty acids namely, oleic acid and linoleic acid were elevated in these patients. Why these fatty acids are increased in MADs remains unknown, but it may be because of oleic and linoleic acid rich-diet. Further studies will be necessary to determine why the level of serum polyunsaturated fatty acids is modified in MADs.

We also found increased levels of acetate and ketone

bodies as well as decreased levels of lipoproteins (mainly VLDL) and saturated fatty acids in MADs. Acetate is the final product of lipid metabolism and its enhancement may indicate an accelerated lipid catabolism (37). Ketone bodies, including acetoacetate and 3-hydroxybutyrate, are catabolized from breaking down fatty acids in liver cell mitochondria and their increase may reflect the utilization of storage lipids (38). Furthermore, decreased VLDL is consistent with elevated lipid degradation in these patients. Overall the observations suggest that lipolysis may be an important source of energy in MADs.

We indicated an elevated level of 3- methyl-2-oxovaleric acid and 3-hydroxyisobutyrate, which are degradation products from isoleucine and valine, respectively. They are so-called branched-chain amino acids (BCAA) which are utilized in the body and muscle protein synthesis. It can be hypothesized that proteolysis of proteins and oxidation of BCAAs have been activated in MADs. In NMR spectra of patients, we showed unusual peaks in valine, isoleucine, and alanine region and reduced levels of these amino acids in patients compared to healthy controls (Figure 1). The most likely explanation for these signals is that the samples are slightly alkaline and also vary in pH very slightly; this gives rise to variable amounts of bicarbonate which can react to form N-carbamates (the amino function reacting with bicarbonate) which have a slightly different chemical shift. The elevated levels of bicarbonates are a result of compensation for chronic respiratory acidosis.

The levels of lysine, glutamate, proline, and hydroxyproline were significantly increased in the serum of MAD patients compared to healthy controls. Since these amino acid residues are found in collagen (39), these results suggest the activation of the collagen breakdown. This finding is consistent with previous studies that have demonstrated that the long-term effect of SM exposure causes an increase in the rate of osteopenia and osteoporosis (40). Osteoporosis is one of the most common causes of corticosteroid therapy that increases osteoblastic suppression and bone resorption (41), as well as loss of bone collagen that occurs in osteoporosis (42). In addition, Sorva *et al.* demonstrated that inhaled corticosteroids decreased carboxy propeptide of type I procollagen which is a marker of bone formation (43). Collagen accounts for more than 90% of the organic bone matrix (43). Since MAD patients were receiving prolonged corticosteroid therapy, our results suggested corticosteroid-induced collagen loss in bone. However, it has been reported that the rate of osteoporosis in MAD patients receiving corticosteroid therapy is higher than asthmatic patients who were treated with the same dose of corticosteroids. Hence, SM-induced osteoporosis has been suggested in these patients (40).

Interestingly, we found that the levels of two more metabolites, citrulline and dimethylamine, increased in serum of MAD patients as compared with healthy controls. It has been shown that exposure to SM elevates serum levels of some pro-inflammatory cytokines such as IL-6 (27), these cytokines increase dimethylarginine dimethylaminohydrolase2 (DDAH2) expression and activity in alveolar type II (ATII) cells (44, 45). DDAHs metabolize asymmetric dimethylarginine (ADMA) and monomethyl arginine (L-NMMA), which is released from methylated proteins by proteolysis, to form L-citrulline and dimethylamine (46). Pullamsetti *et al.* reported that DDAH activation increases fibroblast-induced collagen deposition in an ADMA-independent manner (47). Since methylarginines are endogenous inhibitors of nitric oxide synthase (NOS), this enzyme is subsequently activated by expression and activation of DDAH2. This finding is in agreement with previous studies that showed SM and nitrogen mustard increased NOS2 expression and nitric oxide (NO) production (48, 49). However, the early effect of exposure to mustard gases on NO production has been evaluated in cell cultures and in rats, and it is not clear whether they are relevant to delayed complications of SM in veterans. Prior studies have also shown increased collagen in airway walls in moderate to severe patients exposed to SM (50). It may be suggested that collagen deposition in lungs of these patients has been produced by DDAH activation. Thus, we hypothesized that DDAH inhibition may provide a new therapeutic approach for attenuation of collagen production and subsequently lung injury in MADs.

Conclusion

This work is a global analysis based on metabolomics profiling of human serum by NMR and GC-MS in MAD subjects. In the present study, a robust panel of biomarkers for detecting MADs was established. This panel, consisting of sixteen metabolites detected by NMR and twelve metabolites detected by GC-MS, could differentiate MAD subjects from healthy controls with a higher accuracy. These metabolites are involved in metabolic pathways such as aminoacyl-tRNA biosynthesis, arginine and proline metabolism, and synthesis and degradation of ketone bodies. The serum biomarker panel identified here shows promise as an effective diagnostic tool for MADs, but further investigations are needed to verify our results. Furthermore, in this study, we showed that PCA and OPLS-DA could not only confirm some metabolites that were identified by RF but also could recognize further significant metabolites.

Acknowledgment

The authors thank the individuals participating in this study for their willingness to contribute to the advancement of science. We are also thankful to the

staff of Sasan Hospital, Tehran, Iran. This work is part of the PhD thesis of Bi Bi Fatemeh Nobakht Motlagh Ghoochani at Shahid Beheshti University of Medical Sciences.

Conflict of interest

The authors report no conflicts of interest. The authors alone are responsible for the content and writing of this article.

References

- Javadi M-A, Yazdani S, Sajjadi H, Jadidi K, Karimian F, Einollahi B, *et al.* Chronic and delayed-onset mustard gas keratitis: report of 48 patients and review of literature. *Ophthalmology* 2005; 112:617-625. e612.
- Spoo JW, Monteiro-Riviere NA, Riviere JE. Detection of sulfur mustard bis (2-chloroethyl) sulfide and metabolites after topical application in the isolated perfused porcine skin flap. *Life Sci* 1995; 56:1385-1394.
- Aghanouri R, Ghanei M, Aslani J, Keivani-Amine H, Rastegar F, Karkhane A. Fibrogenic cytokine levels in bronchoalveolar lavage aspirates 15 years after exposure to sulfur mustard. *Am J Physiol Lung Cell Mol Physiol* 2004; 287:L1160-L1164.
- Dompeling E, Jöbsis Q, Vandevijver N, Wesseling G, Hendriks H. Chronic bronchiolitis in a 5-yr-old child after exposure to sulphur mustard gas. *Eur Respir J* 2004; 23:343-346.
- Thomason JW, Rice TW, Milstone AP. Bronchiolitis obliterans in a survivor of a chemical weapons attack. *JAMA* 2003; 290:598-599.
- Ghanei M, Harandi AA. Long term consequences from exposure to sulfur mustard: a review. *Inhal Toxicol* 2007; 19:451-456.
- Aliannejad R, Peyman M, Ghanei M. Noninvasive ventilation in mustard airway diseases. *Respir Care* 2015; 60:1324-1329.
- Sahebkar A, Antonelli-Incalzi R, Panahi Y, Ghanei M, Pedone C. Mustard lung and COPD: common features and treatment? *Lancet Respir Med* 2015; 3:747-748.
- Brindle JT, Antti H, Holmes E, Tranter G, Nicholson JK, Bethell HW, *et al.* Rapid and noninvasive diagnosis of the presence and severity of coronary heart disease using 1H-NMR-based metabolomics. *Nat Med* 2002; 8:1439-1445.
- Srivastava NK, Annarao S, Sinha N. Metabolic status of patients with muscular dystrophy in early phase of the disease: In vitro, high resolution NMR spectroscopy based metabolomics analysis of serum. *Life Sci* 2016; 151:122-129.
- Yang J, Chen T, Sun L, Zhao Z, Qi X, Zhou K, *et al.* Potential metabolite markers of schizophrenia. *Mol psychiatry* 2013; 18:67-78.
- Jain M, Nilsson R, Sharma S, Madhusudhan N, Kitami T, Souza AL, *et al.* Metabolite profiling identifies a key role for glycine in rapid cancer cell proliferation. *Science* 2012; 336:1040-1044.
- Nobakht M, Gh BF, Aliannejad R, Rezaei-Tavirani M, Taheri S, Oskouie AA. The metabolomics of airway diseases, including COPD, asthma and cystic fibrosis. *Biomarkers* 2014; 20:5-16.
- Nobakht M, Gh BF, Arefi Oskouie A, Rezaei-Tavirani M, Aliannejad R, Taheri S, Fathi F, *et al.* NMR spectrometry-

- based metabolomic study of serum in sulfur mustard exposed patients with lung disease. *Biomarkers* 2016; 22:413-419.
15. Nobakht BF, Aliannejad R, Rezaei-Tavirani M, Arefi Oskouie A, Naseri MT, Parastar H, et al. NMR-and GC/MS-based metabolomics of sulfur mustard exposed individuals: a pilot study. *Biomarkers* 2016; 21:479-489.
16. Vestbo J, Hurd SS, Agustí AG, Jones PW, Vogelmeier C, Anzueto A, et al. Global strategy for the diagnosis, management, and prevention of chronic obstructive pulmonary disease: GOLD executive summary. *Am J Respir Crit Care Med* 2013; 187:347-365.
17. Eilers PH. Parametric time warping. *Anal Chem* 2004; 76:404-411.
18. Skov T, van den Berg F, Tomasi G, Bro R. Automated alignment of chromatographic data. *J Chemom* 2006; 20:484-497.
19. Tomasi G, van den Berg F, Andersson C. Correlation optimized warping and dynamic time warping as preprocessing methods for chromatographic data. *J Chemom* 2004; 18:231-241.
20. Nielsen N-PV, Carstensen JM, Smedsgaard J. Aligning of single and multiple wavelength chromatographic profiles for chemometric data analysis using correlation optimised warping. *J Chromatogr A* 1998; 805:17-35.
21. Nicholson JK, Foxall PJ, Spraul M, Farrant RD, Lindon JC. 750 MHz ¹H and ¹H-¹³C NMR spectroscopy of human blood plasma. *Anal Chem* 1995; 67:793-811.
22. Xu WF, Upur H, Wu YH, Mamtimin B, Yang J, Ga YJ, et al. Metabolomic changes in patients with chronic obstructive pulmonary disease with abnormal Savda syndrome. *Exp Ther Med* 2015; 9:425-431.
23. Kapoor S, Clay E, Wallace GR, Fitzpatrick M, Bayley R, Young SP. *Metabolomics in the analysis of inflammatory diseases: INTECH Open Access Publisher*; 2012.
24. White JR, Harris RA, Lee SR, Craigon MH, Binley K, Price T, et al. Genetic amplification of the transcriptional response to hypoxia as a novel means of identifying regulators of angiogenesis. *Genomics* 2004; 83:1-8.
25. Albina JE, Henry W, Mastrofrancesco B, Martin B-A, Reichner JS. Macrophage activation by culture in an anoxic environment. *J Immunol* 1995; 155:4391-4396.
26. Scannell G. Leukocyte responses to hypoxic/ischemic conditions. *New horizons (Baltimore, Md)* 1996; 4:179-183.
27. Attaran D, Lari SM, Towhidi M, Marallu HG, Ayatollahi H, Khajehdaluae M, et al. Interleukin-6 and airflow limitation in chemical warfare patients with chronic obstructive pulmonary disease. *Int J Chron Obstruct Pulmon Dis* 2010; 5:335-340.
28. Arroyo CM, Broomfield CA, Hackley BE. The role of interleukin-6 (IL-6) in human sulfur mustard (HD) toxicology. *Int J Toxicol* 2001; 20:281-296.
29. Arroyo C, Schafer R, Kurt E, Broomfield C, Carmichael A. Response of normal human keratinocytes to sulfur mustard (HD): cytokine release using a non-enzymatic detachment procedure. *Hum Exp Toxicol* 1999; 18:1-11.
30. Nobakht M, Gh BF, Oskouie AA, Aliannejad R, Rezaei-Tavirani M, Tavallaie S, Baghban AA, et al. Pro-oxidant-antioxidant balance in Iranian veterans with sulfur mustard toxicity and different levels of pulmonary disorders. *Drug Chem Toxicol* 2015; 39: 362-366.
31. Tappia PS, Dent MR, Dhalla NS. Oxidative stress and redox regulation of phospholipase D in myocardial disease. *Free Radic Biol Med* 2006; 41:349-361.
32. Storm C, Danne O, Ueland PM, Leithner C, Hasper D, Schroeder T. Serial plasma choline measurements after cardiac arrest in patients undergoing mild therapeutic hypothermia: a prospective observational pilot trial. *PloS One* 2013; 8:e76720.
33. Balsinde J, Balboa MA, Insel PA, Dennis EA. Regulation and inhibition of phospholipase A2. *Annu Rev Pharmacol Toxicol* 1999; 39:175-189.
34. Ray R, Legere R, Majerus B, Petrali J. Sulfur mustard-induced increase in intracellular free calcium level and arachidonic acid release from cell membrane. *Toxicol Appl Pharmacol* 1995; 131:44-52.
35. Lefkowitz LJ, Smith WJ. Sulfur mustard-induced arachidonic acid release is mediated by phospholipase D in human keratinocytes. *Biochem Biophys Res Commun* 2002; 295:1062-1067.
36. Sorenson DK, Kelly TM, Murray DK, Nelson DH. Corticosteroids stimulate an increase in phospholipase A2 inhibitor in human serum. *J Steroid Biochem* 1988; 29:271-273.
37. Kumari S, Tishel R, Eisenbach M, Wolfe AJ. Cloning, characterization, and functional expression of acs, the gene which encodes acetyl coenzyme A synthetase in *Escherichia coli*. *J Bacteriol* 1995; 177:2878-2886.
38. Wolfe R, Shaw J, Durkot M. Energy metabolism in trauma and sepsis: the role of fat. *Prog Clin Biol Res* 1982; 111:89-109.
39. Keshari KR, Zektzer AS, Swanson MG, Majumdar S, Lotz JC, Kurhanewicz J. Characterization of intervertebral disc degeneration by high-resolution magic angle spinning (HR-MAS) spectroscopy. *Magn Reson Med* 2005; 53:519-527.
40. Agin K, Rajae A, Mehrabi M, Darjani HRJ, Ghofrani H. Osteoporosis among asthmatic patients exposed to mustard gas compared with non-exposed asthmatics. *Tanaffos* 2004; 3:7-11.
41. Picado C, Luengo M. Corticosteroid-induced bone loss. *Drug safety* 1996; 15:347-359.
42. Shuster S. Osteoporosis, a unitary hypothesis of collagen loss in skin and bone. *Med Hypotheses* 2005; 65:426-432.
43. Sorva R, Turpeinen M, Juntunen-Backman K, Karonen S-L, Sorva A. Effects of inhaled budesonide on serum markers of bone metabolism in children with asthma. *J Allergy Clin Immunol* 1992; 90:808-815.
44. Shahar I, Fireman E, Topilsky M, Grief J, Kivity S, Spirer Z, et al. Effect of IL-6 on alveolar fibroblast proliferation in interstitial lung diseases. *Clin Immunol Immunopathol* 1996; 79:244-251.
45. Ueda S, Kato S, Matsuoka H, Kimoto M, Okuda S, Morimatsu M, et al. Regulation of cytokine-induced nitric oxide synthesis by asymmetric dimethylarginine role of dimethylarginine dimethylaminohydrolase. *Circ Res* 2003; 92:226-233.
46. Ogawa T, Kimoto M, Sasaoka K. Occurrence of a new enzyme catalyzing the direct conversion of NG, NG-dimethyl-L-arginine to L-citrulline in rats. *Biochem Biophys Res Commun* 1987; 148:671-677.
47. Pullamsetti SS, Savai R, Dumitrascu R, Dahal BK, Wilhelm J, Konigshoff M, et al. The role of dimethylarginine dimethylaminohydrolase in idiopathic pulmonary fibrosis. *Sci Transl Med* 2011; 3:87ra53-87ra53.
48. Gao X, Ray R, Xiao Y, Ishida K, Ray P. Macrolide antibiotics improve chemotactic and phagocytic capacity as well as reduce inflammation in sulfur mustard-exposed monocytes. *Pulm Pharmacol Ther* 2010; 23:97-106.

49. Gao X, Ray R, Xiao Y, Barker PE, Ray P. Inhibition of sulfur mustard-induced cytotoxicity and inflammation by the macrolide antibiotic roxithromycin in human respiratory epithelial cells. *BMC Cell Biol* 2007; 8:17.

50. Ghanei M, Tazelaar HD, Chilosi M, Harandi AA, Peyman M, Akbari HMH, *et al.* An international collaborative pathologic study of surgical lung biopsies from mustard gas-exposed patients. *Respir Med* 2008; 102:825-830.